International Journal of Sciences and Techniques of Automatic control & computer engineering
IJ-STA, Special Issue, CEM, December 2008, pp. 652–669.

On Reactive Power Control of Power Systems Including Wind Energy and Unified Power Flow Controller

Houda Brahmi, Rachid Dhifaoui

Unit Research on Power System and Electrical Machines (RME)
National Institute of Applied Sciences and Technology (INSAT)
Centre Urbain Nord, BP 676, 1080 Tunis Cedex
Rachid.Dhifaoui@insat.rnu.tn

Abstract. *Electricity interruption gives rise to a complete disorder in the society and is therefore unappreciated and highly criticized. Consequently, it becomes a great concern for national and/or private energy companies to conduct their power systems under severe requirements. These companies are asked to ovoid failures that induce power oscillation, voltage drop and high frequency deviations because these phenomena can produce the loss of the system integrity by rapid voltage collapse or any transient stability mechanism. New technology alternatives such as FACTS (flexible alternative current transport systems) can positively support conventional control systems such as PSSs (power system stabilizer), AVRs (automatic voltage regulator) and TGs (turbine governor). But at the same time, it is to recognize that power system control becomes more complicate and requires suitable global strategies. The paper deals with this problem and aims to show that UPFC is a suitable device in particular to reinforce variable wind energy penetration in the power system. This is on one hand. On the other hand it is shown in this work that UPFC can become very constraining for synchronous machines in absence if adequate AVRs.*

Key words. *Power systems, Transfer capability, Voltage control, Wind energy, Unified power flow controller, Injection model*

1. Introduction

In our modern societies, electric energy consumption becomes practically the primer to-life need. In fact, throughout the world, energy demand is in very fast growth and citizens become very sensitive to the continuous availability of electricity at required voltage magnitude and frequency.
Electricity interruption, for any reason, gives rise to a complete disorder in the society and is therefore unappreciated. Consequently, it becomes a great concern for national and/or private energy companies to conduct their power systems under severe

This paper was recommended for publication in revised form by the editor Staff.
Edition: CPU of Tunis, Tunisia, ISSN: 1737-7749

requirements. These companies are asked to ovoid failures that induce power oscillation, voltage drop and high frequency deviations. These phenomena can produce the loss of the system integrity by rapid voltage collapse or any transient stability mechanism [1, 2]. It is well known that the great failures that have severely touched large scale power networks are related to insufficient transfer capability and inadequate or absent control processes. Thus, electric energy companies implement various control systems as PSSs (power system stabilizer [3]), AVRs (automatic voltage regulator [4]), TGs (turbine governor [5]) and SVCs (static var compensator [6]). Unfortunately, these conventional control processes become insufficient for large scale modern power networks including in particular wind energy sources [7, 8]. Such energy is by nature variable with wind speed that is variable with geography. Very complicate transient phenomena can be effectively excited by the presence of aero generators. Thus, more efficient and powerful control systems are needed. In this point of view, take place new technological control systems labelled FACTS (flexible alternative current transport systems). The most efficient configuration of FACTS is the shunt-series control solution known as UPFC (unified power flow controller [9, 10]).

Phenomena encountered in power systems are very complicate and need very high background in technology components, physics and mathematics. Engineers of electric companies should in fact solve various related difficult problems such as constrained and optimal load flow [11], dynamic and static voltage collapse calculation [12], transient stability analysis including numerical solution and eigenvalues sensitivity of dynamical systems [13, 14], bifurcation points [15, 16], adequate transfer functions and controllers gains computation [17], and so on. Theses activities are crucial to understand and investigate power systems phenomena and therefore to design and install appropriate control schemes.

In this paper, we will discover and comment a very complicate problem related to dynamic control of reactive power. The considered power system includes classical synchronous machines and loads, a wind energy source, AVR systems and a UPFC. It will be shown in particular that if voltage magnitude of synchronous machines is not well controlled, the UPFC device becomes a severe reactive load for these machines.

Section 2 of the paper presents the dynamical model of the synchronous machine conjointly with power system algebraic equations. Section 3 gives the considered structure of AVRs and develops their differential equations. Then, section 4 briefly introduces the model of the wind energy source. The great developments will be presented in section 5 that deals with the injection model [18] of the UPFC. The power balance of the system is investigated and all necessary equations to introduce the principle of power injection model are presented and commented. PQ generators are then defined to describe the UPFC device. The control of these generators is presented and discussed in section 6. Finally, section 7 is reserved to illustration. All the necessary data of the power system under study are given and the results are commented.

In terms of modelling, we deal with a mathematical model composed by differential and algebraic equations (DAE) [19] as indicated by equations (1.1) and (1.2). Algebraic variables y correspond to voltage magnitudes and phases. Dynamic x are

associated to the systems state variables and include for example synchronous machine speed and transient emfs. They also include control variables as those of TGs and AVRs variables. Variable p can model an external perturbation parameter introduced for particular topic.

$$\begin{cases} \dfrac{dx}{dt} = f(x,y,p) & (1.1) \\ 0 = g(x,y,p) & (1.2) \end{cases}$$

These DAEs are solved by a trapezoidal NR-based technique with possible variable time integration step. At each step, say h, one uses the initial condition (x_o, y_o) to generate the new point (x,y) by solving simultaneously (1.3) and (1.4) considering the parameter p constant during the step.

$$\begin{cases} x - x_o - \dfrac{h}{2}[f(x_o,y_o,p) + f(x,y,p)] = 0 & (1.3) \\ g(x,y,p) = 0 & (1.4) \end{cases}$$

The global Jacobian matrix of this system is built as given by (1.5) where sub matrices J_{fx} , J_{fy}, J_{gx} and J_{gy} are matrices of partial derivatives of f and g with respect to x and y. Sub matrix I is the identity matrix with the same dimensions as x. To reduce time computing, sparse matrices techniques are very useful in the iterative NR process.

$$J = \begin{bmatrix} I - \dfrac{h}{2} J_{fx} & -\dfrac{h}{2} J_{fy} \\ J_{gx} & J_{gy} \end{bmatrix} \quad (1.5)$$

2. Synchronous machine model

Synchronous machines are here described by a fourth order model describing dynamics of rotor angle, rotor speed and direct and quadrature components of the stator internal transient emf. Machine emf and terminal current and voltage are expressed in a synchronously rotating reference frame linked to a selected slack bus. We use conventional notations and refer the reader to [20] for example. In this context, mechanical motion of the synchronous machine is expressed by differential equations (2.1) and (2.2) where P_M and P_G hold respectively for input mechanical power and output electric power. Parameters ω_b, H and D define respectively the base frequency of the power system, inertia time constant and damping coefficient of the synchronous generator. Variable ω_r is the per unit machine speed. Dynamics behaviour of machine transient emf are given by equation (2.3) and (2.4) characterizing the flux decay phenomenon. Voltage and current components, machine active power P_G and reactive power Q_G are given by algebraic equations (3.1)-(3.6).

$$\begin{cases} \dfrac{d\delta_r}{dt} = \omega_b(\omega_r - 1) & (2.1) \\ \dfrac{d\omega_r}{dt} = \dfrac{P_M - D(\omega_r - 1) - P_G}{2H} & (2.2) \\ \dfrac{dE_d^{'}}{dt} = \dfrac{-E_d^{'} + (X_q - X_q^{'})I_q}{T_{qo}^{'}} & (2.3) \\ \dfrac{dE_q^{'}}{dt} = \dfrac{E_{fd} - E_q^{'} - (X_d - X_d^{'})I_d}{T_{do}^{'}} & (2.4) \end{cases}$$

$$\begin{cases} E_d^{'} - R_s I_d + X_q^{'} I_q - V_d = 0 & (3.1) \\ E_q^{'} - X_d^{'} I_d - R_s I_q - V_q = 0 & (3.2) \\ V_d I_d + V_q I_q - P_G = 0 & (3.3) \\ V_q I_d - V_d I_q - Q_G = 0 & (3.4) \\ P_G - E_d^{'} I_d - E_q^{'} I_q - (X_d^{'} - X_q^{'}) I_d I_q = 0 & (3.5) \\ Q_G - E_q^{'} I_d + E_d^{'} I_q + X_d^{'} {I_q}^2 + X_q^{'} {I_d}^2 = 0 & (3.6) \end{cases}$$

It is to note that as mentioned above, mechanical power P_M and direct field voltage E_{fd} are kept constant during transient. Note also that this model is written for every synchronous machine i present the power system. Therefore, these equations are to be added to power balance equations at machine terminal bus as follows.

$$\begin{cases} P_G + p(t) - P_{Load} - \sum PLines = 0 & (3.6) \\ Q_G - Q_{Load} - \sum QLines = 0 & (3.7) \end{cases}$$

3. The AVR model

Voltage magnitude of the synchronous machine is assumed controlled by IEEE-Type-1 AVR whose structure is given by Fig.A1 in Appendix. This structure includes five blocs:

- a time delay bloc associate with voltage measurement system,
- a principal function generating voltage control signal v_{r1} ,
- a excitation circuit producing the field voltage v_f ,
- a voltage filtering bloc with signal v_{r2} ,
- a non linear ceiling function $S_e(v_f)$ sketching saturation phenomenon.

According to this, the AVR structure is described by the set of following differential equations [21 to 24]:

$$\begin{cases} \dfrac{dV_m}{dt} = \dfrac{V - V_m}{T_r} & (4.1) \\ \dfrac{dv_{r1}}{dt} = \dfrac{K_a\left(V_{ref} - V_m - v_{r2} - \dfrac{K_f}{T_f}v_f\right) - v_{r1}}{T_a} & (4.2) \\ \dfrac{dv_{r2}}{dt} = \dfrac{-\dfrac{K_f}{T_f}v_f - v_{r2}}{T_f} & (4.3) \\ \dfrac{dv_f}{dt} = \dfrac{v_{r1} - \big(1 + S_e(v_f)\big)v_f}{T_e} & (4.4) \end{cases}$$

The ceiling function is expressed as follows:

$$S_e(v_f) = A\left(e^{B v_f} - 1\right) \quad (4.5)$$

It is important to note that field voltage v_f is equal to variable E_{fd} introduced in equation (2.4) of the synchronous machine model given in the previous section: $(v_f = E_{fd})$.

4. Wind energy source model

We here consider a simplified model for wind energy sources. Detailed models can be found in the literature [12, 14]. Let us recall that available wind energy generators around the world are in great part standard squirrel cage and doubly fed asynchronous machines. For these machines, active power is expressed in terms of a rotor resistance variable versus machine sleep frequency. So for simplicity, we represent these generators as sketched by Fig.1 where parameters $\bar{z}_w$ and jX_w illustrate rotor transient impedance and stator magnetizing reactance.

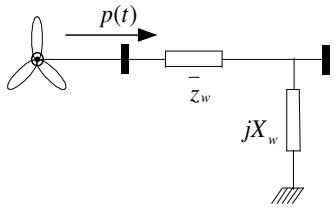

Fig.1. The wind energy generator model

The stator transient impedance can be included in the transmission line connected to the generator. Energy extracted from the wind is characterized by a variable active power injection $p(t)$. The frequency adaptation problem is assumed realized by fast

and ideal invertors. The variable $p(t)$ is taken dynamically slow as compared to the power system variables. This assumption permits to consider $p(t)$ constant during the integration step used while solving DAEs. We obtain consequently a sufficiently stable integration process. The active power injection $p(t)$ is added step by step to buses power balance.

5. The power injection model of the UPFC

The general configuration of the UPFC is shown by Fig.2. The device has a shunt transformer T1 driven from the bus and a series transformer T2 injected in the line. These two transformers are coupled by two inverters that are separated by a DC link. The capacitor is controlled so that some active power quantity is extracted by inverter C1 from the bus and injected by inverter C2 in the transmission line via transformer T2. In terms of reactive power, the control is more flexible in the sense that inverter 1 can works as generator as well as receiver. Through the series part, the reactive power balance is also relatively easy to establish.

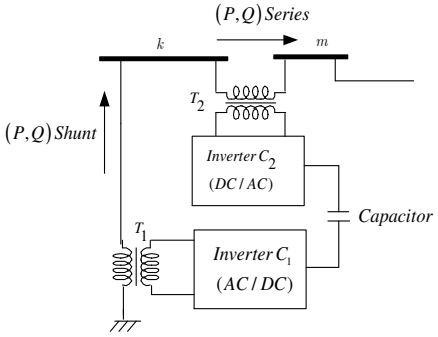

Fig.2. General structure of an UPFC

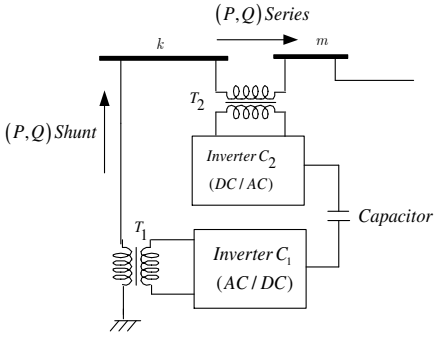

Fig.2. General structure of an UPFC

UPFC has the ability to adjust simultaneously the bus voltage magnitude, the transmission line reactance and the transited power or current flow. Therefore, all classic solutions of shunt (as SVC: static var compensator) or STATCOM (static compensator) and series as TSCS: thyristor controlled series capacitor) compensation processes are present in the UPFC. We here present the injection model [18] and bring out in the best possible way the mechanism of energy transit between the two branches of the device. Then, we establish a simple and reliable control scheme that ensures suitable convergence to a very adequate steady state operating point.

First, let us indicate by k and m respectively the input bus and the output bus between them the UPFC is placed. We note by jx_T the transformer reactance (resp. $-jb_T$ the admittance) of the series part of the UPFC device. As the main function of the series branch of the UPFC is to inject in the transmission line an AC voltage with controllable magnitude and phase, we consider an ideal series voltage source $\overline{v}_T$ delivering to the receiving bus m the current $\overline{I}_{km}$ through the reactance jx_T. The shunt branch is driven from bus k and has the function to inject active power P_{sh} and reactive power Q_{sh} quantities. In this point of view, we consider Fig.3 to illustrate this model widely used in literature.

Implementation of this model conjointly with available software packages presents serious difficulties. In fact, power systems simulation programs are based on only shunt energy sources where zero voltage is linked to ground point. Thus, including series energy sources in these packages requires fundamental transformations. To overcome this problem, a solution based on equivalent power injection model is proposed in [18]. This approach replaces the model of Fig.3 by that of Fig.4. The equivalence between these two circuits is based on the duality between Thevenin's voltage generator and Norton's current generator. The problem returns to establish values of P_k, Q_k, P_m and Q_m.

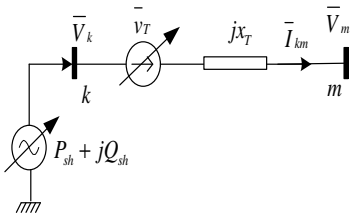

Fig.3. The physical model of the UPFC

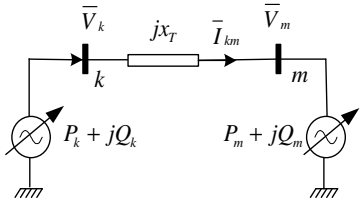

Fig.4. The injection equivalent model of the UPFC

Let $\overline{V}_k = V_k e^{j\theta_k}$ and $\overline{V}_m = V_m e^{j\theta_m}$ be the voltage vectors of the input port and output port respectively. Angles θ_k and θ_m are computed with respect to the slack bus reference frame rotating at the fundamental frequency. The series branch is governed by the two equivalent following equations:

$$\overline{V}_k + \overline{v}_T = jx_T\overline{I}_{km} + \overline{V}_m \quad (5.1)$$

$$\overline{I}_{km} = -jb_T\overline{v}_T - jb_T(\overline{V}_k - \overline{V}_m) \quad (5.2)$$

In the sense of equation (5.2), the current of the series branch is viewed as a current generator $\overline{i}_T = -jb_T\overline{v}_T$ in parallel with admittance $-jb_T$ of the transformer as sketched by Fig.5.

Using this equivalence solves computation of the different injection powers of equivalent UPFC circuit given by Fig.4. Without loss of generality but for more convenient mathematical formulation, we consider that series voltage source $\overline{v}_T$ has an angle γ with respect to a reference frame transported by the voltage vector $\overline{V}_k$ of the input bus k as indicated by Fig.6. Consequently, with respect to the reference bus bar of the network, $\overline{v}_T$ is expressed as $\overline{v}_T = v_T e^{j(\theta_k+\gamma)}$ and in the reference frame of $\overline{V}_k$ it is noted $\overline{v}_T = v_T e^{j\gamma} = v_{TD} + jv_{TQ}$. In the remaining part of the paper we consider this frame of work and we set:

$$\overline{v}_T = v_{TD} + jv_{TQ} = v_T(\cos\gamma + j\sin\gamma) \quad (6)$$

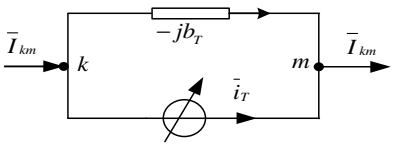

Fig.5. Parallel Norton's equivalent current

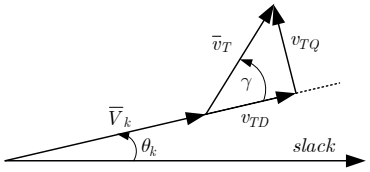

Fig.6. Definition of the series voltage source vector

The Norton's current source $\overline{i}_T$ produces at ports k and m two injected power quantities defined as follows:

$$P_{Nk} = b_T V_k v_{TQ} \quad (7.1)$$

$$Q_{Nk} = b_T V_k v_{TD} \quad (7.2)$$

$$P_{Nm} = -b_T V_m(v_{TQ}\cos\theta_{km} + v_{TD}\sin\theta_{km}) \quad (7.3)$$

$$Q_{Nm} = -b_T V_m(v_{TD}\cos\theta_{km} - v_{TQ}\sin\theta_{km}) \quad (7.4)$$

$$\theta_{km} = \theta_k - \theta_m \quad (7.5)$$

The series voltage source $\overline{v}_T$ supplies apparent complex power defined by:

$$P_S = b_T V_m\,(v_{TD}\sin\theta_{km} + v_{TQ}\cos\theta_{km}) - b_T v_{TQ} V_k \quad (8.1)$$

$$Q_S = b_T V_m \left(v_{TQ} \sin\theta_{km} - v_{TD} \cos\theta_{km}\right) + b_T\left(v_{TD} V_k + {v_T}^2\right) \qquad (8.2)$$

Assuming that the UPFC structure is lossless and with respect to the actual circuit of Fig.3, active power control should impose $P_{sh} = P_S$. So to pass to the virtual equivalent circuit of Fig4, we state:

$$P_k = P_{sh} + P_{Nk} = P_S + P_{Nk} \qquad (9.1)$$

$$P_m = P_{N\mathrm{m}} \qquad (9.2)$$

Reactive power control of the shunt branch is realized independently of that of active power. So, in similar way, the reactive power equivalence between Fig.3 and Fig.4 implies:

$$Q_k = Q_{sh} + Q_{Nk} = Q_{sh} + Q_{Nk} \qquad (10.1)$$

$$Q_m = Q_{Nm} \qquad (10.2)$$

Input and output active and reactive power injections of the equivalent model described by Fig.4 are finally governed by:

$$P_k = b_T V_m \left(v_{TD} \sin\theta_{km} + v_{TQ} \cos\theta_{km}\right) \qquad (11.1)$$

$$P_m = -P_k \qquad (11.2)$$

$$Q_k = Q_{sh} + b_T v_{TD} V_k \qquad (11.3)$$

$$Q_m = b_T V_m \left(v_{TQ} \sin\theta_{km} - v_{TD} \cos\theta_{km}\right) \qquad (11.4)$$

Note finally that the output port of the UPFC supplies a transmission line. The previous developments naturally hold if we integrate the reactance of the line in the reactance of the transformer.

6. The considered UPFC control strategy

Let us first consider simple control laws such as those indicated by equations (13.1) and (13.2) to command the components of the series voltage source of the UPFC.

$$\frac{dv_{TQ}}{dt} = \frac{v_{TQ}^{ref} - v_{TQ}}{\tau_V} \qquad (12.1)$$

$$\frac{dv_{TD}}{dt} = \frac{v_{TD}^{ref} - v_{TD}}{\tau_V} \qquad (12.2)$$

As well known, the maximum power flow through a classical transmission line (without UPFC) varies in opposite sense with the line reactance. Thus, a admitted

solution to enhance transfer power capability is to reduce this reactance. Decreasing x_T reduces reactive losses and can ensure a positive effect on transient stability phenomenon. Fixed capacitor or variable capacitor with switched thyristor lies in this solution. This function can be also realized by UPFC if we impose to it to establish a compensation ratio η_x of the transport line reactance. To be sure that the UPFC realizes this function and emulates therefore a capacitor, the components of the series voltage source should be linked to those of the transported current by the following equalities.

$$v_{TD}^{ref} = -\eta_x x_T I_Q \tag{13.3}$$

$$v_{TQ}^{ref} = \eta_x x_T I_D \tag{13.4}$$

Note that all components are reported in the reference frame of the input port voltage. The reference values being taken variable with the current line, the UPFC will have an internal constant reactance. On the other hand, components of the series voltage should respect dimensional limits. We impose therefore to dynamics of these components to respect the following constraints of upper and lower limits.

$$v_{\min} \leq v_{TD} \leq v_{\max} \tag{14.1}$$

$$-\sqrt{{v_{\max}}^2 - {v_{TD}}^2} \leq v_{TQ} \leq \sqrt{{v_{\max}}^2 - {v_{TD}}^2} \tag{14.2}$$

Furthermore, it is important not only to consider voltage limits but also to take into account reasonable limit on the power flow. The active power that departs from the input port to the output port is given by:

$$P_{km} = b_T V_k V_m \sin\theta_{km} + b_T V_k v_{TQ} \tag{15.1}$$

This equation shows that the presence of the UPFC introduces a power deviation ΔP (the second right term) with respect to the base case without this device (the first right term). In this study, we consider a limitation ratio η_p :

$$\left| \frac{\Delta P}{P_{km} - \Delta P} \right| \leq \eta_p \tag{15.2}$$

This returns to consider the following constraint on the quadrature component of the series injected voltage source. This new constraint is treated simultaneously with constraints (14.1) and (14.2).

$$-V_m \left|\sin\theta_{km}\right| \leq v_{TQ} \leq V_m \left|\sin\theta_{km}\right| \tag{15.3}$$

Now, we return to the shunt branch of the UPFC. We attribute to this branch to control the voltage level at the input port by an integrator with anti wind up limiters. Thus, the dynamics of the reactive power to inject in the bus is governed by:

$$\frac{dQ_{sh}}{dt} = K_V \left(V_{ref} - V\right) \tag{16.1}$$

$$-Q_{\max} \leq Q_{sh} \leq Q_{\max} \tag{16.2}$$

7. Simulations and comments

The structure of the test system is depicted on Fig.A2 in Appendix. It is composed by 9 buses, 4 transformers, 4 lines, 4 constant loads, a wind energy generator G1 placed at bus 1 and 3 synchronous machines G2, G3 and G4 placed at buses 7, 8 and 9 respectively. Bus 9 is used as common reference for voltage vectors (slack bus). The UPFC will be place in the line connecting buses 3 and 4. The input port is bus 4. All parameters and data of initial steady state operating point are given by Tables 1, 2 and 3 reported in Appendix. They are considered in pu with respect to 100 MW power base. All DAEs are solved by PSAT [24] package except models of the UPFC and the wind energy generator. These two models are built separately from PSAT. At each step integration time, we get necessary values of voltages and currents from PSAT and we solve independently these two models. The result is then injected in PSAT and the process continues. Two main points are investigated in simulations.

First, we investigate the general validity of theoretical developments on UPFC and the proposed control strategy. This will be achieved by a perturbation scenario built as follows. The power system is working in steady state, the power of the wind generator is set to a constant of 0.5 pu and the UPFC is out of use. At t=2 sec, the UPFC is commanded according to the control strategy presented in the previous section. The shunt branch of the UPFC is ordered to regulate voltage magnitude of bus 4 at 1.05 pu while the series branch is commanded to establish an equivalent series capacitor of 30% of the line reactance under a limitation of 20 % on active power deviation. Then, at t=20 sec the power of the wind energy source is increased linearly by a ramp of 0.025 pu per second until t=40 sec.

Table 5 of the Appendix reports initial load flow. It shows that bus 4 has the most low voltage magnitude which explains the choice to place UPFC beside this bus. After applying the UPFC device, the voltage level is highly reinforced as reported by Table 6 giving the new steady state load flow taken at t=60 sec. Colons 4 and 5 of this table show also that the final power balance of active and reactive power of the UPFC is respectively about 0.16 pu and 1. pu.

Some results of the transient regime are summarized by Fig.8 to Fig.12. We observe the normal convergence of all variables to their new steady state values. No undesirable oscillation phenomenon is encountered. Evolution of voltage magnitudes of synchronous machines (buses 7, 8 and 9) is given by Fig.8. The suitable convergence is obtained which proves that AVRs have realized the demanded function. The shunt reactive power and the series active power of the UPFC device are given by Fig.9. The reactive power is positive which implies that it is really injected in bus 4. In contrary, the active power is negative which implies that it is extracted from bus 4. Voltage magnitude at bus 4 is well regulated at 1.05 pu as demanded. Fig.10 shows the dynamic evolution of this voltage. It is also important to note that UPFC has effectively realized the function of line reactance compensation. This is confirmed by Fig.11 giving the transited reactive power by the line 4-3; that power changes of sign.

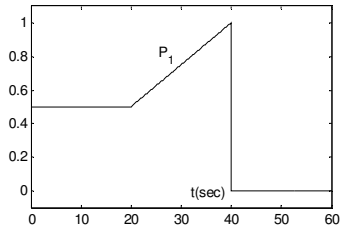

Fig.7. The wind energy variation process

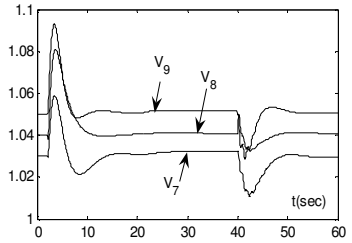

Fig.8. Voltage magnitudes of synchronous machines

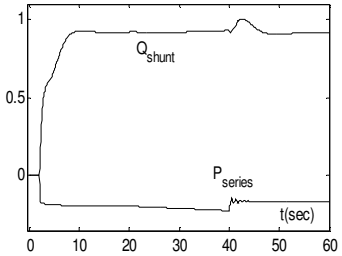

Fig.9. Active power and reactive power the UPFC

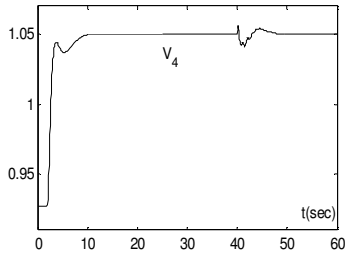

Fig.10. Voltage magnitude at input port of the UPFC

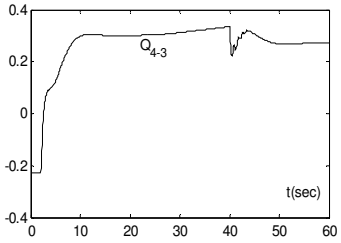

Fig.11. Reactive power of line 4-3

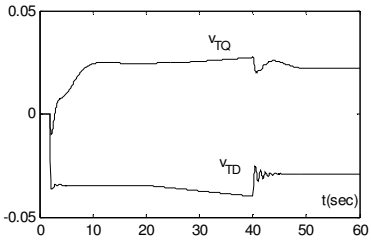

Fig.12. Components of series voltage of the UPFC

In this second part of simulations we describe and comment some complicate problems observed in dynamic control of reactive power. We analyse the effect of reactive power control on voltage dynamics result. For more clarification of the discussed problem, we will discard the series part of the UPFC and we only consider reactive power control by the shunt branch. This branch is commanded to increase the voltage magnitude of bus 4 from 0.9269 pu to 1.05 pu. The problem will be studied

in two cases; with and without AVRs functions. The active power delivered by the wind generator is maintained constant 0.5 pu.

Fig.13 and Fig.14 gives respectively voltage magnitude of bus 4 and reactive power of the shunt branch of the UPFC in presence of AVRs. The voltage is well controlled and the UPFC shunt branch works as reactive power generator. Total reactive power generation of the synchronous machines is 3.4594 pu distributed respectively as [0.7389 1.1387 1.5818] pu.

Now, if we disconnect AVRs and repeat the operation of voltage control at bus 4, we observe that the voltage control is again well achieved (Fig.15). However, contrary to the first situation, new steady state of reactive power is negative (Fig.16) which means that the shunt branch of the UPFC works as receiver. Total reactive power generation of the synchronous machines is 4.8785 pu distributed respectively as [0.8872 1.7361 2.2552] pu. Without AVRs, the reactive power balance increases therefore by 1.4191 pu.

On the other hand, if the reactive power of the shunt branch is forced to remain positive as indicated by Fig.17 and AVRs are set out of service, the voltage control fails and we obtain a dangerous voltage increase at all buses as shown by Fig.18. Observe here that the system is integrated until t=60 sec. At this time, total reactive generation of synchronous machines is 4.1496 pu distributed as [0.4360 1.584 2.1296]. Evolution of rotor angles corresponding to this case is shown by Fig.17.

First, the fact that the voltage of bus 4 increases and at the same time the bus is absorbing reactive power (when ARVs are out of use) is surprising in a way.
The well known rule is exactly the contrary. If one desires to enhance bus voltage magnitude he should supply this bus by reactive power. Surely, this holds in static control. Here, because terminal voltages of machines vary freely from any control, multiple reactive power flows can take place. Thus, controlling voltage in some limited regions and ignoring machines bus bars can force these machines to produce excessive reactive power which is constraining.

The second point that merits to be discussed is the problem of excessive voltage magnitude increase when the reactive power injection is locked to zero at certain moment of the transient. It is first to note that there is no doubt that the obtained regime is a stable steady state as proved by negative signs of real parts of eigenvalues shown by Fig.18. We believe in the existence of multiple regions of attraction of equilibrium points. Also, the fact that loads are here considered constant can contribute to voltage alleviation to satisfy algebraic load flow equations. Surely, it is an open interesting problem to investigate in details and carefully.

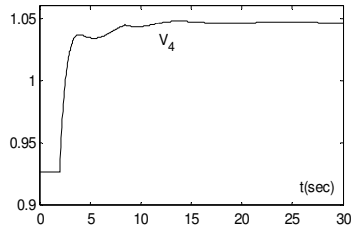

Fig.13. Voltage magnitude at bus 4 (AVRs in use)

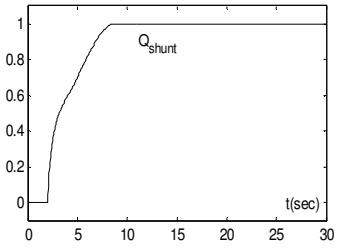

Fig.14. Shunt reactive power of the UPFC

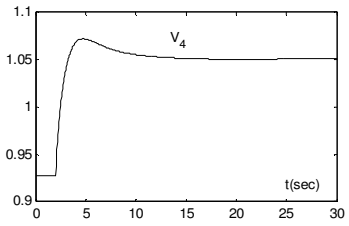

Fig.15. Voltage magnitude at bus 4

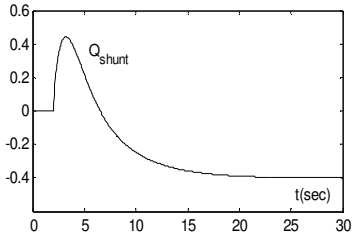

Fig.16. Shunt reactive power of the UPFC

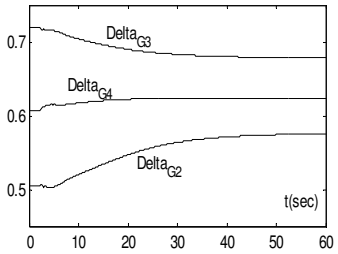

Fig.17. Rotor angles in case of positive anti wind up limiter of shunt reactive power

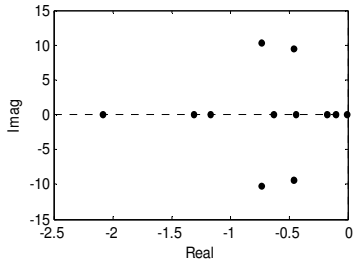

Fig.18. Eigenvalues in case of positive anti wind up limiter of shunt reactive power

8. Conclusion

This study is carried out in the context of large power systems including variable power injection as wind energy generation, classical voltage control as AVRs and new technology control as UPFC. Simplified but realistic models are considered for synchronous machines and wind energy sources. AVRs are IEEE-type1. The UPFC model is treated with respect to the principle of power injection equivalent sources. All necessary equations are presented and commented. The study is concretized by

simulation of a didactic power system. Obtained results largely confirm the high capabilities of the UPFC to control voltage level and to compensate a sufficient ratio of the associate energy transmission line. The device works well even in highly variable injected power level.

Two surprising regimes are discovered. The first concerns the fact that in absence of AVRs, UPFC can become a severe reactive load for synchronous machines. The second point concerns the existence of an equilibrium point with voltage level also in the case when AVRs are out of use. This equilibrium is obtained if we inject some reactive power and then we reset it to zero. These points merit to be studied carefully and in details.

References

[1] G. Anderson and all: "Causes of 2003 major grid blackouts in North America and Europe and recommended means to improve system dynamic performance", IEEE Trans. On Power Systems, Vol.20, No.4, 2005.

[2]: Marija Ilic and all: "Preventing future blackouts by means of enhanced electric power systems control: from complexity to order", Proceedings of the IEEE, Vol.93, No.11, 2005.

[3] Scott Greene, Ian Dobson, Fernando L. Alvarado: "Decentralized stability enhancement control of synchronous generator", IEEE Trans. On Power Systems, Vol.15, No.4, 2000.

[4] Zwe-Lee Gaing: "A particale Swarm optimization approach for optimum design of PID controller in AVR system", IEEE Trans. On Energy Conversion, Vol.19, No.2, 2004.

[5]: Haibo Jiang, Hongzhi Cai, John F. Dorsey, Zhihua Qu: "Toward a globally robust decentralized control for large scale power systems", IEEE Trans. On Control Systems Technology, Vol.5, No.3, 1997.

[6] Claudio A. Canizares, Zeno T. Faur: "Analysis of SVC and TCSC Controllers in Voltage Collapse", IEEE Trans. On Power Delivery, Vol.14, No.1, 1999.

[7] J. Marques, H. Pinheiro, H. A. Grundling, J. R. Pinheiro, H. L. Hey: "A survey on variable speed wind turbine system", in Congresso Braseleiro de Electronica de Potencia, (COBEP), Brazil, 2003.

[8] V. Akhmatov, H. Knudsen, A. H. Nilson, J. K. Pederson, N. K. Poulsen: "Modelling and transient stability of large wind farms", Electrical power and energy system 25, Elsevier science 2003.

[9] Z. T. Faur: "Effects of FACTS devices on static voltage collapse phenomenon", Thesis of University of Waterloo, Ontario, Canada, 1996.

[10] K. R. Padyar, A. M. Kulkarni: "Control Design and Simulation of Unified Power Flow Controlle", IEEE Trans. On Power Delivery, Vol.13, No.4, 1998.

[11] Federico Milano, Claudio A. Canizares, Marco Invernizzi: "Multiobjective optimisation for pricing system security in electricity market", IEEE Trans. On Power Systems, Vol.18, No.2, 2003.

[12] Scott Greene, Ian Dobson, Fernando L. Alvarado: "Sensitivity of the loading margin to voltage collapse with respect to arbitrary parameters", IEEE Trans. On Power Systems, Vol.12, No.1, 1997.

[13] IEEE/CIGRE Joint Task Force on Stability Terms and Definitions: "Definition and classification of power system stability", IEEE Trans. On Power Systems, Vol.19, No.2, 2004.

[14] Ian Dobson, Emilio Barocio: "Scaling of normal form analysis coefficients under coordinate change", IEEE Trans. On Power Systems, Vol.19, No.3, 2004.

[15] Luonan Chen, Kazuyuki Aihara: "Stability and bifurcation analysis of differential algebraic equations", IEEE Trans. On Circuits and Systems, Vol.48, No.3, 2001.

[16] Saffet Ayasun, Chika O. Nawankpa, Harry G. Kwatny: "Computation of singular and singularity induced bifurcation points of differential algebraic power system model", IEEE Trans. On Circuits and Systems, Vol.51, No.8, 2004.

[17] Rodrigo A. Ramos, André C. P. Martins, Newton G. Bretas: "An improved methodology for design of power system damping controllers", IEEE Trans. On Power Systems, Vol.20, No.4, 2005.

[18] M. Ghandhari: "Control Lyapunov function: A control strategy for damping of power oscillations in large power systems", Thesis of the Royal Institute of Technology, Stockholm, Sweden, 2000.

[19] R. E. Mahony, L. M. Mareels: "Global solution for differential/algebraic systems with implications for Lyapunov direct stability methods", Journal of Mathematical Systems, Estimation and Control, Vol.5, No.4, 1995.

[20] R. Dhifaoui, H. Brahmi, O. Hasnaoui, F. Bacha: "Investigation of the unstable orbit of fourth order model of one machine infinite bus system", GESTS Int. Trans. On Computer Science and Engineering, Vol.26, No.1, 2006

[21] F.L. Alvarado, J. Meng, C.L. DeMarco, W.S Mota" Stability Analysis of interconnected power systems coupled with market dynamics", IEEE Transaction On Circuits and Systems, Vol.14, No.2,1999.

[22] Yannis L. Karnavas, Demetrios P. Papadopoulos: "Excitation control of a synchronous machine using polynomial neural networks", Journal of Electrical Engineering, Vol.55, No.7-8, 2004.

[23] Jan Murgas, Andrej Dobrovic, Eva Miklovicova, Jozef Dubravsky: "Two Level Turbogenerateur Control System", Journal of Electrical Engineering, Vol..55, No.3-4, 2004.

[24] Federico Milano: "An Open Source Power System Analysis Toolbox", IEEE Trans. On Power Systems, Vol.20, No.3, 2005.

Appendix

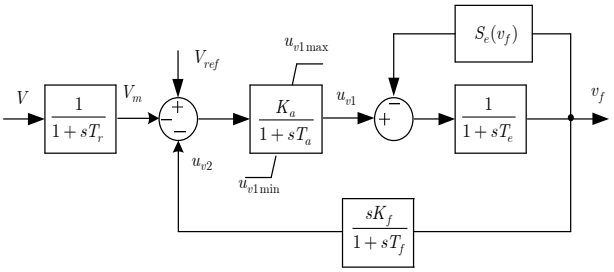

Fig.A1: Structure of the used AVRs

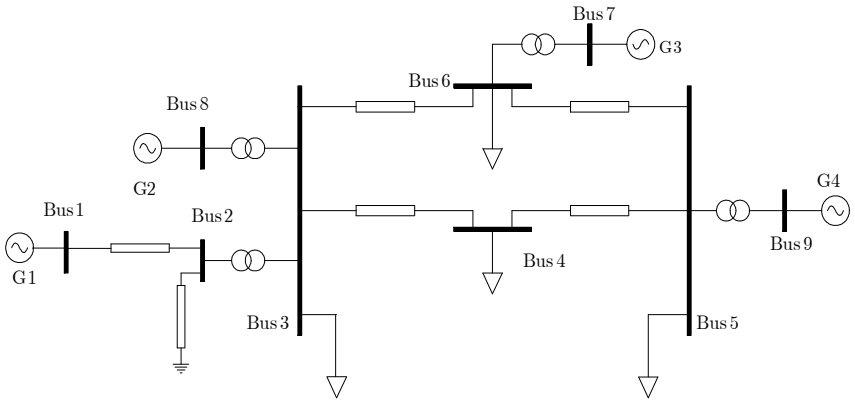

Fig.A2: Structure of studied power system

Table 3: Parameters of the UPFC

$v_{\max} = 0.2$	$K_V = 3$
$Q_{sh\max} = 1$	$Q_{sh\min} = -1$
$\tau_V = 0.1$	$\tau_Q = 0.2$
$\eta_x = 0.3$	$\eta_p = 0.2$

Table 1: Reactances of lines and transformers

From Bus	To Bus	X(pu)
1	2	0.0200
2	3	0.1000
3	4	0.2000
3	6	0.1667
3	8	0.0333
4	5	0.2000
5	6	0.2000
5	9	0.0333
6	7	0.0333

Table 4: Parameters of AVRs

	G2	G3	G4
$v_{r\max}$	5	5	5
$v_{r\min}$	-5	-5	-5
K_a	400	400	400
T_a	0.1	0.1	0.1
K_f	0.45	0.45	0.45
T_f	1	1	1
T_e	0.001	0.001	0.001
A	0.0006	0.0006	0.0006
B	0.9	0.9	0.9
V_{ref}	1.0347	1.0459	1.0562

Table 2: Parameters of synchronous machines

	G2	G3	G4
$S_n(MVA)$	300	300	300
$V_n(KV)$	230	230	230
$f_n(Hz)$	60	60	60
X_d	1.77	1.88	1.59
$X_d{}'$	0.33	0.275	0.349
X_q	1.48	1.69	1.36
$X_q{}'$	0.53	0.44	0.579
$T_{do}{}'$	5	6.4	2.88
$T_{qo}{}'$	1.095	0.72	1.08
D	2	0	2
H	6	4.5	5

Table 5: Initial load flow of the power system without UPFC

Bus	V(pu)	(°)	PG(pu)	QG(pu)	PL(pu)	QL(pu)
1	0.97814	5.241	0.5	-	-	-
2	0.97819	4.6422	-	-	-	-
3	0.98983	1.6821	-	-	2	1
4	0.92688	-7.7378	-	-	1	0.5
5	0.98663	-4.6135	-	-	3	1.5
6	1.0036	4.0927	-	-	1	0.5
7	1.03	7.7906	2	0.88041	-	-
8	1.04	5.3955	2	1.6302	-	-
9	1.05	0	2.5	2.0968	-	-

Table 6: Load flow of the power system with UPFC

Bus	V(pu)	(°)	PG(pu)	QG(pu)	PL(pu)	QL(pu)
1	0.9989	-0.6216	0.5	-	-	-
2	0.9989	-0.6216	-	-	-	-
3	1.0089	-0.6216	0.1634	0.0893	2	1
4	1.0500	-9.0145	-0.1634	1.0328	1	0.5
5	1.0032	-4.7653	-	-	3	1.5
6	1.0074	3.9276	-	-	1	0.5
7	1.0296	8.0694	2	0.7669	-	-
8	1.0407	3.2487	2	1.0631	-	-
9	1.0505	0	2.5	1.6022	-	-